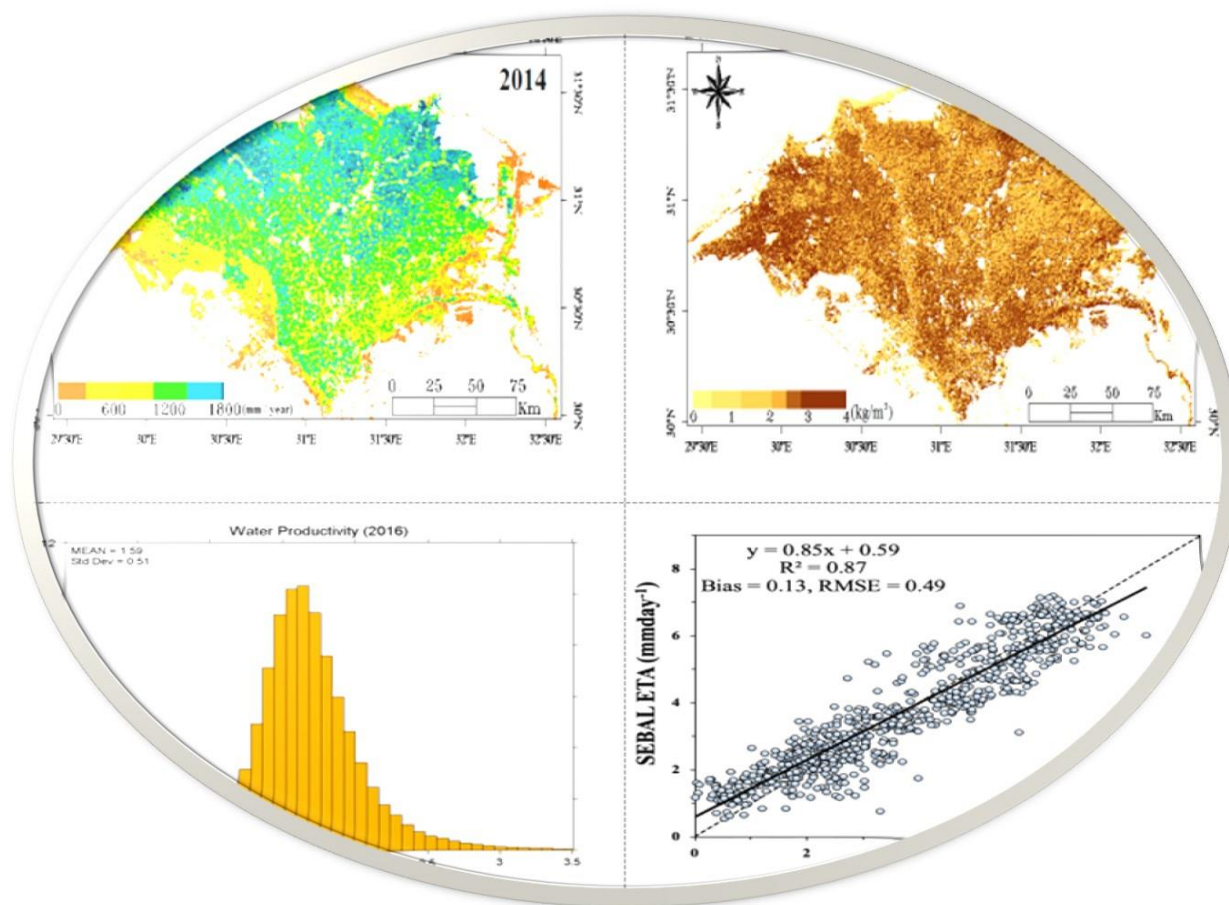# Enhancing agricultural water productivity in the irrigated areas of Nile Delta through innovative science-based solution

Report submitted by

International Center for Agricultural Research in the Dry Areas (ICARDA)

Report submitted to

CGIAR Research Program on WLE (CRP 5)

January 2020

Table of Contents

1. Summary

Actual evapotranspiration (ET_a), including surface evaporation and plant transpiration, is required to understand both hydrological and ecological processes between the land surface and the atmosphere. Reliable spatio-temporal distribution of ET_a is crucial to demonstrate the hydrological status of complex landscapes for water resources planning and monitoring, efficient irrigation scheduling, and climate change research. Due to complex land-plant-atmosphere interactions and natural variability in topography, soil moisture, and vegetation type, estimation of ETa is the most challenging among all of the components of the hydrologic cycle, especially in regions where water is scarce or fluctuates seasonally.

The continuously emerging availability of high-resolution satellite imagery at affordable prices, or even free of charge, has made water flux information derived from Remote Sensing (RS), specifically Evapotranspiration (ET), a reliable source for water accounting of agricultural water use over large areas (e.g., sub-national, national or basin level).

In fact, remotely-sensed water-accounting products are currently getting implemented in various Ministries of the focus countries of the Near East and North Africa (NENA) Water Scarcity Initiative (WSI) and at the same time beneficiary of the Sida Project on "Implementing the 2030 Agenda for water efficiency/productivity and water sustainability in NENA countries" (GCP/RNE/009/SWE).

Some databases of ET at operational spatial and temporal scales are being made publicly available for several regions of the world, including the NENA Region. For Example; FAO Water Productivity Open-access portal (WaPOR), ET Ensemble (IHE-Delft), GloDET (Water for Food, Daugherty Global Institute, Nebraska) and OpenET (https://etdata.org/ under preparation); Simplified Surface Energy Balance (SSEB), USGS/NASA . Meanwhile local institutions also generate their own databases using models like SEBAL (Surface Energy Balance Algorithm for Land) or METRIC (Mapping Evapotranspiration at high Resolution with Internalized Calibration). However, the weak point of all these databases is that they suffer from a general limited and scattered field validation and, more specifically, virtually no validation at all in the NENA Region.

If water accounting has to provide the evidence base for a strategic planning of water resources, if large-scale crop water-productivity gaps needs to be benchmarked and monitored, if water conservation strategies have to be developed based on water consumptive limits, then RS ET determinations needs to carry over acceptable degree of accuracy.

To define the accuracy of RS ET data, a comparison with field actual ET measurements is required. This comparison will not only serve to define the accuracy of RS ET data but also to provide the opportunity for calibrating and validating RS algorithms calculating ET_a.

The overarching objective is to establish and operate a Regional Network of specialized Institutions, within the five countries of reference, to conduct field measurements of actual ET, over selected crops and for at least two crop seasons, in order to evaluate the accuracy of existing RS based ET estimates.

As this project is being implemented in Egypt, Jordan, Lebanon, Morocco, and Tunisia, some national institutions such as IAV and INGRAF generating ET_a using well known energy balance system algorithms e.g., SEBAL (Surface Energy Balance Algorithm for Land), METRIC (Mapping Evapotranspiration at high Resolution with Internalized Calibration), SEBS (Surface Energy Balance System), unfortunately suffering from a general limitation of scattered field validation and, virtually no validation at all in the NENA Region. Therefore, the ET_a measurements established from the CORDOVA stations network could effectively be used to validate the ET_a in the field and to use the measured data to calibrate the remote sensed based estimations.

The regional network has been established by setting up communications and agreements with participating countries. These agreements included the terms of references and field activities to be implemented. We have agreed with all partner is to unify the crop and method of measurement using CORDOVA system as standard protocol. Parallel to the standard protocol of ET measurement, double check with other protocols such as energy balance and lysimeter are also used to calibrate the CORDOVA station to make sure about the accuracy and reliability of collected data.

2. Introduction

Actual evapotranspiration (ETa) is a major component of the water cycle. Estimating ETa of crops is critical for several applications in the management of water resources: to derive water productivity, to deploy water accounting, to strategically plan water resources, to operate irrigation, etc.

With the continuous emerging of freely-available high-resolution satellite imageries, agricultural water management is offered the potential to obtain ETa from Remote Sensing (RS), and therefore addressing large areas and reducing enormously the costs of ETa determinations. However, the RS ETa determinations need to have a degree of accuracy (or uncertainty) commensurate to the scale (e.g. farm, national, basin, etc.) and type of application for which ETa data are used (e.g., irrigation scheduling, crop water productivity, national water accounting, basin-level water allocation, etc.).

To define the accuracy of RS ETa data, a comparison with field (or ground) crop ETa measurements is required. Moreover, this comparison will provide the opportunity for calibrating and validating RS algorithms calculating ETa. However, measuring field ETa is not an easy task and several methods exist, each one with its own degree of sophistication, skills requirement of the operator, area-sampling representativeness (single point, some m2, ha, etc.), accuracy and costs. A further not-easy task is the comparison itself, between 'RS ETa' and the 'field ETa', due to the mismatch between the 'area-sampling representativeness' of the field method and the 'ground resolution' of the RS determination.

ICARDA is in charge of coordinating, operating and backstopping the members of the NENA-ETNet, and this report represents a "standard protocol" of methods and procedures of field ETa measurements that will be adopted by the members of the Regional Network. It will serve as a guideline for the participating country managers, scientists, technicians and field operators involved in the Regional Network.

3. Actual evapotranspiration by satellite remote sensing

Among the various energy budget components which are responsible for the water movement within the surface and Earth's atmosphere, the comprehensive information of both latent (LE) and sensible (H) heat fluxes together with the soil moisture content, are pivotal to several various environmental and natural applications, as well as the observations of crop water requirement and consumption, growth and productivity of plants, along with development and management framework of irrigation networks (Brutsaert, 1982; Gowda et al., 2008; Su et al., 2005). The accuracy of the models used in weather forecasting can also be significantly improved by using the information of turbulent fluxes in the modelling of crucial atmospheric and hydrological process (Hwang and Choi, 2013). Furthermore, the quantitative and qualitative data on these parameters is exceedingly vital for scrutinizing of desertification and land degradation on a large scale (Ershadi et al., 2014a; Fisher et al., 2008). Since the water movement through land plant and atmosphere interaction is strongly linked with the land use changes, therefore planning and management of land use patterns are closely related for the sustainable water resources (Allen et al., 1998). There are several variations in the factors such as climate, human interventions along with the land use changes which strongly affect the water cycle. Thus, estimating the energy and water budget above plant's canopies is very important for understanding the water cycles, as well to improve the accuracy and of models which could be deployed for quantifying and enhancing the agricultural productivity at regional scales (Singh et al., 2008; Teixeira et al., 2009).

In developing countries which have entirely agriculture-based economies, frequent modifications in land use land cover (LULC) system are witnessed regulated with the rapidly growing populations. Two major categories in LULC changes are normally fall in modification and conversion whereas the conversion is the change from one land use category to another category, however, modification is the change, due to functional and physical attribute, within a category of land cover and use. These drastic changes in LULC framework has drastic impact on soil water and moisture contents, biodiversity and on the environment, which ultimately impacting the food and fibber production from the agricultural (Allen et al., 1998). That's why a better understanding of impacts of changes in land cover on the movement of water cycle will also help

policy makers to define approaches for minimizing the undesirable impacts of the future changes in land use and cover.

The key process of removing water from a watershed is evaporation and the process by which water removed from the crop or plant surface or any other living surface which contains water contents is known as transpiration. Thus, evapotranspiration (ET) is an important component of water cycle and primarily based on the combine process of both evaporation and transpiration. Being the single biggest flux of outgoing water from the Earth's surface; the accurate ET characterization of ET is very crucial to advance our better understanding of a range of climatic, ecosystem and hydrological processes and is useful in various applications, e.g., monitoring of drought, water resource management, application of hydrological model, weather forecasts and improving the growth in agricultural system (Li et al., 2009; Senay et al., 2011). ET on regional basis is accounted for more than half of the rainfall while in semi-arid areas, it is nearly equal to rainfall . Thus, it is very crucial to acquire a deep understanding of the LULC and the hydrological cycle interactions by accurately quantifying the ET. However, it is the one of the most difficult water cycle components to map or characterize especially at large spatial scale varying from an irrigation scheme to a regional or continental level for strategic assessment of water resources management considering the impact of land use changes on those available water resources (Liaqat and Choi, 2015b; Liou and Kar, 2014; Wang and Dickinson, 2012).

The field-based instruments which utilized for measurement of H, LE fluxes and soil moisture, provides certain advantages. There are also several conventional approaches exist such as Bowen ratio (BR), Weighing Lysimeter, and Eddy Covariance (EC) measurements which can be applied at point scale to any land use system for the measurement of energy budget fluxes (Gowda et al., 2008; Kalma et al., 2008; Li et al., 2009). On the other hand, the employment of ground-based instruments is often costly, laborious and sometimes subjected to instrumentation error while only able to provide localized measurement of soil moisture and surface energy fluxes. Another major problem with all existing conventional approaches is that they either have the scientific limitation or could be very expansive to extend their quantification to large regional spatial and temporal scale especially in the regions with variability of climatic conditions. This is because these traditional techniques are more applicable over the homogeneous area where they provide the

accurate measurement of ET. However, their accuracy also reported to be compromised due to land surface heterogeneity and complex hydrological process as well as the requirement of several land surface components limits their estimations of ET to large spatial scale (Byun et al., 2014). Integrated ancillary field knowledge with imageries of remote sensing is mostly able to give synoptic and repetitive views of essential components characterizing soil moisture, interaction of land and surface, and surface energy fluxes and for this purpose several approaches have been developed using the remote sensed data.

In the past few decades, the advances in remote sensing has made it possible to figure out which system can provide spatially explicit information of surface fluxes on large spatio-temporal scale. To map ET patterns at meso and reginal scale on Earth's surface, satellite remote sensing imaginary have offered promising source of data and the direct link establishes with the help of surface temperature between parameters of Earth energy balance and surface radiation (Allen et al., 2011; Byun et al., 2014; Gowda et al., 2013). Due to their ability to give synoptic and repetitive views on spatial scale without any disturbance and associability problem of the surveyed area, remote sensing approaches become attractive for retrieval of these crucial components (McCabe et al., 2011). Therefore, several approaches have been developed using freely and often available date from several types of remote sensing imageries whereas the methodologies of those approaches is mostly based on the combination ancillary atmosphere and surface measurements to estimate the surface energy and water budget components. The variation in soil moisture status and other surface water fluxes have been evident by combined use remote sensed data from thermal and optical infrared radiometers. Thermal infrared remote sensed data has been indicated as useful for analysing the biophysical characteristics of the landscape as well as modelling of the ecological processes in the landscape (Boegh et al., 2009). These techniques vary from purely numerical techniques to more physical-based techniques on the basis of equation of energy balance and knowledge acquired from the "scatter plot" relationships of vegetation indices or the crop metrics and surface radiant temperature estimations. These critical atmospheric and surface variables are fed as forcing parameters to simulate ET and surface fluxes based on the energy equilibrium equation. To retrieved land surface temperature (LST), atmospheric temperature and vegetation indices, the data embedded in thermal infrared, near infrared and visible band can be used while

the remote sensing approach offers a continuous and large spatial scale coverage rather quick with in no time and in most cases free of cost. Land surface fluxes estimated with remote sensing offers the robust measurement from a resolution range from several km^2 to few cm^2 from certain satellites (Tasumi et al., 2005).

Satellite remote sensing also offers the continuous spatial scale data for surface albedo, Normalized Difference Vegetation Index (NDVI), surface emissivity, radiometric surface temperature and Laef Area Index (LAI), most of them essential for approaches and models which partition the available energy. During past few decades, many efforts has been made to incorporate the surface temperature by remote sensing along with other crucial parameters e.g. albedo and VI into the ET modelling (Liaqat et al., 2016). As a result, many satellite-based ET models has been developed varying in mechanism, including input and output parameters and their advantages and limitations. Hence, for the better understanding of the computational mechanisms involved among different methodologies the rundowns and comparisons of distinctive remote sensing-based ET model is essential to choose a particular model for wider scientific application in the fields of water resources management. Few examples among the several approaches developed recently are reviewed and explained frequently by several studies; for example (Choi et al., 2011; Li et al., 2006), The survey of progress in crop evapotranspiration modelling and estimation with focused on the particular aspects of irrigation interest has provided by (Ershadi et al., 2014b).

Foundation to the evapotranspiration estimation was laid by Penman, (1948) who originated a relationship between outgoing water flux and the meteorological parameters. After that in 20's century, a substantial development was made in process of evapotranspiration with energy balance concept. The conventional way to measure the ET requires the meteorological data for the numerical equations and model simulations. However, these approaches cannot effectively represent the ET at a large scale due to complexity in land cover and topography. At present the penman-Monteith equation is most commonly used method to estimate the ET, but this method is not applicable at regional scale due to heterogeneity and this is also regarded as point scale method which may be not practically able to estimate at large spatial scale. To address the reason of applicability over a much larger scale the remote sensing approaches have been developed to quantify the ET for shorter time duration.

3.1. Algorithms for estimating actual evapotranspiration

The remote sensing methods for estimating evapotranspiration are based on the concept of energy balance which used the principal parameters derived from the net radiation (Awan et al., 2016; Choi et al., 2011; Liaqat and Choi, 2015a). Several energy balance algorithms have been developed in the recent advancement of satellite remote sensing which are being employed to quantify the crop water consumption. Although the developed algorithms have been tested in numerous ecosystems across the different parts of the globe by several scientist and reported their satisfactory performance but there is still some degree of uncertainties exist in computation of ET. The widely used single source surface energy balance algorithms has been reviewed in this report to pin point the merits and demerits of the famous methodologies in spatio-temporal quantification of land surface ET.

3.1.1 SEBAL

The Surface Energy Balance Algorithm for Land (SEBAL) was developed in the Netherlands by (Bastiaanssen, 2000; Bastiaanssen et al., 1998) which is a spatial scale image-processing model based on the residual of the surface energy balance for the quantification of ET across different land use system. The SEBAL was designed to estimate the all the components of energy budget at both local and regional scales by utilizing the minimum ground-based information, and yet is considered the most promising model currently available within the framework of similar approaches used to estimate ET. This model requires physical parameterization to use with the empirical relationships designed with its intermediate approach which require the digital image information gathered from the satellite remote sensing system measured in the visible, near-infrared, and thermal infrared radiation, which is further converted to the land surface temperature and vegetation indices. The SEBAL model operates on each pixel basis in the imagery for the computation of first net radiation (Rn) from the balance of short and longwave radiation which was then further used to estimate the latent heat flux (LE) as a residual of the energy balance equation.

The SEBAL model used a generic equation proposed for the estimation of soil heat flux (G) that is applicable to all sorts of soil type and land use cover (Bastiaanssen, 2000; Bastiaanssen et

al., 1998). This model has justified its performance not only at field scale showing an accuracy of 85% and 95% at daily and seasonal scales, respectively in several ecosystem worldwide but also on catchment as well on regional scale (Ahmad et al., 2005; Awan et al., 2016). In all of the models which are based on energy budget equation, the most difficult part is the estimation of sensible heat flux (H) which involves the complex solutions of various parameters to solve the residual energy balance. In general, to compute the sensible heat flux, the SEBAL model used two different condition for the air temperature located at two different height levels, such as h1 a height which should be close to the surface while the h2 which is usually an upper height depending upon the crop and meteorological condition of the area. The SEBAL model then consider homogeneous meteorological and land surface conditions to determine the value of temperature gradient dT for each pixel in the image by assuming the existence of a linear relationship between dT and the radiometric surface temperature Ts such as given below:

$$dT = aTs + b \qquad (1)$$

where dT is the near-surface air temperature difference, "a" and "b" are empirical coefficients obtained from the so-called "anchor" pixels for a given satellite image and T_s is the radiometric surface temperature (Teixeira et al., 2009). Generally, the two extreme anchor pixels i.e., most wet and most dry pixels in entire area of study represent conditions of extreme evaporative behaviour within the image. For example, at a "wet (cold)" pixel, the most of the available energy ($R_n - G$) is assumed to be consumed by the evaporation consequently dT assumed to be near zero ($dT_{wet} = 0$) which results zero the sensible heat flux (H) for that corresponding pixel. On the other hand, evaporation is close to zero at a "dry (hot)" pixel where all the available energy is essentially adapted into the sensible heat. The aerodynamic theory for the two extreme anchor pixel conditions is then utilized by the model to compute the near surface air-temperature difference, dT (Teixeira et al., 2009) as follows:

$$dT_{dry} = \frac{H_{dry} \times r_{a\,dry}}{\rho_{air\,dry}\,C_p} \qquad (2)$$

where H_{dry} (sensible heat flux for the dry anchor pixel W·m-2) and is equal to ($R_n - G$).

The coefficients "a" and "b" in Equation (1) can be effectively assessed, once the surface-air temperature differences for both the extreme condition (i.e., hot and cold anchor pixels) is determined. These coefficients "a" and "b", are then utilized in an iterative setup in the model to develop a linear gradient of the surface-air temperature difference dT for each pixel of the image by using land surface temperature in Equation (2). In SEBAL model, the hot pixel is chosen from an image pixel which is representing an area with least vegetation or displays high surface temperature, while the cold pixel is generally choose from a pixel located in well-watered crop conditions assuming no stress conditions. With the user defined extreme anchor pixels, the sensible heat flux is usually calculated iteratively with corrected roughness length for the stability, while this procedure also required an extrapolation of wind speed from ground level to a height of about 100 to 200 m. Usually, the identification of wet pixels are easily spotted over an area of well-watered surfaces or over a relatively large, calm water surface, whereas recognizing the dry pixels is the foremost vital perspective in SEBAL. Apart from the reasonably well accuracy of the SEBAL model, its overall known to be very contextual in terms of anchor pixel selection as reported in a recent study (Singh et al., 2008; Timmermans et al., 2007), as they stated that some time depending upon short area of interest the non-existence of extreme condition may not fully justify the assumption of the model which are required to trigger the SEBAL model appropriately.

The major focal points of SEBAL for the quantification of land surface fluxes from the thermal remote sensing information are (1) least utilize of supporting ground-based meteorological and land use information; (2) programmed inside correction of uncertainties in the image dataset, which avoids strict rectification of atmospheric impacts on surface temperature; and (3) inner calibration, which is usually performed by the model internally for each processed image. Other than its several points of interest, it has a few disadvantages as well. Major drawbacks of this approach are that (1) to decide demonstrate parameters a and b which are requirement of the subjective identification of extreme hot/dry and wet/cool pixels inside the image are required (Bastiaanssen, 2000; Bastiaanssen et al., 1998; Timmermans et al., 2007). Any errors in the selection of extraordinary anchor pixel which could be induced by the inefficient expert of the model, variation in the domain size of the area of interest, or by the varying spatial resolution of the satellite sensor may also largely compromise the resulting estimations of H flux and ET from

the SEBAL (Bastiaanssen et al., 1998); (2) based on the digital elevation model of the area, a few alterations are also need to incorporate in the model to consider the lapse rate adjusted for the land surface temperature and wind speed (Awan and Ismaeel, 2014); (3) Evaluated H is significantly influenced by the errors or mistakes induced in the surface-air temperature difference or uncertainties in computation of surface temperature measurements from the remote sensing data could largely affect the estimation of sensible heat flux and consequently the final map of ET; and (4) there is also need to carefully incorporate the effect of radiometer viewing angle which can trigger variation by several degrees in land surface temperature estimations.

3.1.2 METRIC

Mapping evapotranspiration at high Resolution with Internalized Calibration (METRIC) is an energy balance model and a variant of SEBAL. The ground based meteorological information is used to estimate the reference ET in integration with the original SEBAL model to derive the actual ET in METRIC model. Overall, METRIC is a comprehensive image processing model which derive the actual ET as a residual of the energy budget on the Earth's surface over homogeneous as well as on complicated surfaces. The underlying fundamental concept of METRIC model is based on using the satellite remote sensing data of thermal infrared, visible and near-infrared spectral region along with ground based meteorological measurements of wind speed and air temperature along with land use information to estimate the evaporating moisture contents as indicated by the (Allen et al., 1998; Allen et al., 2007). Similar to SEBAL model, the computation of sensible and latent heat flux also based on the selection of two extreme anchor pixel which is usually observed in the processing image in order to define the boundary conditions of energy budget for that particular image. The METRIC model used an internal calibration which removes the need of atmospheric correction of the satellite data such as reflectance and surface temperature measurements which are required for other similar type of models (Allen et al., 2007). The major benefits of these internal calibration are that the impact of biases which are normally contributed from the remote sensing data for the assessment of aerodynamic or surface roughness is reduced.

For the internal calibration the wet and dry anchor pixel are manually selected from the underlying image which are used to describe the linear temperature gradient above land surface

condition. Similar to SEBAL the dry anchor pixel is typically representing the dry bare agriculture field where ET is normally 0 providing all available energy to the sensible heat flux. However, this model differed from SEBAL in terms that wet pixel is considered usually from a well-irrigated field where ET = reference ET value of a standardized alfalfa crop having no stress and unlimited water condition.

However, a recent study (Allen et al., 2011; Allen et al., 2013; Awan et al., 2016) questioned the context-dependency of these models (i.e, METRIC and SEBAL), as the fundamental existence of extreme anchor pixel conditions may not necessarily exit in a particular image which are required to force those models. Thus, the quantified ET from these contextual models may have large uncertainties if the extreme condition is not properly set. Considering this limitation, the developers have improved the methodologies of these models over time, such as an automated selection of extreme conditions have been introduced basis on extent of area of interest, climatic parameters, spatial resolution and underlying land use conditions. Furthermore, the proper selection of automatic pixel in METRIC model helps in accommodating the varying effect of fractional vegetation cover on the ET extremes (Liaqat and Choi, 2015a).

The METRIC model has been successfully tested over several hetero- homogeneous land surface across different parts of the globe and studies have been reporting the model performance with reasonable accuracy. Santos implemented the METRIC by integrating with a water balance model in Spain in order to provide the significant improvements in the irrigation scheduling(Santos et al., 2008). Liaqat and Choi (2015a) compared the estimated ET with the lysimeter measurements in the semi-arid region of US and pointed out the high potential for successful ET estimates of both SEBAL/METRIC models.

3.1.3 SEBS

The Surface Energy Balance System (SEBS) is another well-known energy budget model which was developed by Su et al. (2005). SEBS is modified version of SEBI and used to estimate the turbulent land surface fluxes by combining the routinely available meteorological data and satellite remote sensing information. The main bases of the SEBS are to drive the evaporative fraction based on energy balance at limiting cases by calculating the roughness length for heat

transfer as well as by computations of other land surface physical parameters (Ershadi et al., 2014b). Like other energy budget models, the SEBS model define two (wet and dry) limiting boundary conditions but without contextual identification, such as at dry limit the latent heat flux is assumed to be zero where sensible heat flux values reach to its maximum point (i.e., $H_{dry} = R_n - G$) and can be estimated by using equation (3). However, at the wet limit, the evaporation is limited only by the available energy depending upon the particular atmospheric and land surface condition, and ET reached to its potential rate (LE_{wet}), with minimum value for the sensible heat flux, H_{wet} (equation 4) The sensible heat flux at both boundary condition can be expressed as follows:

$$H_{dry} = R_n - G \tag{3}$$

$$H_{wet} = \frac{(R_n - G)\gamma}{(\gamma + \Delta)} - \frac{\rho C_p (e_{sat} - e)}{r_a(\gamma + \Delta)} \tag{4}$$

where r_a is dependent on the Obukhov length, which in turn is a function of the friction velocity and sensible heat flux. Then, the relative evaporative fraction (EF_r) and evaporative fraction (EF) can be expressed as:

$$EF_r = \frac{H_{dry} - H}{H_{dry} - H_{wet}} \tag{5}$$

$$EF = \frac{EF_r \times LE_{wet}}{R_n - G} \tag{6}$$

The SEBS model made a distinction between the PBL/Atmospheric Boundary Layer (ABL) and the Atmospheric Surface Layer (ASL) by utilizing similarity theory. Such distinction is made to take the ABL height is used as a reference of potential air temperature to calculate the turbulent heat fluxes where the discrepancy is created to account the difference between surface temperature and potential air temperature. The SEBS model used the ground-based meteorological measurements and remote sensing derived land surface parameters as the forcing inputs. SEBS performance has been reported reasonably well over several land use surface across the globe.

Jia et al. [81] validated the SEBS performance by comparing the estimated sensible heat flux which was estimated by using ground data from a Numerical Weather Prediction and remote sensing data from ATSR with large aperture scintillometers. Liaqat et al. (2015) compared the performance of SEBS estimated heat fluxes and ET with eddy covariance measurements situated in four different types of land use in Northeast Asia as well as the results from SEBS and METRIC were compared.

However, the absolute errors in the potential air temperature and in estimates of land surface temperature can largely contribute to the potential errors in the estimation of sensible heat flux due to a lack of internal calibration in SEBS (Liaqat et al., 2015). Overall, the results from the above studies showed the usefulness of SEBS in estimating the land surface fluxes in varying land use conditions. Daily, monthly, and annual estimation of evaporation in a semi-arid environment have been done by SEBS. Furthermore, the easy to operate assumption of SEBS allow its application for both field scale and regional scale application under different atmospheric stability regimes with as high accuracy as 10%–15% compared to that of in-situ measurements but mostly for the high ranged of 0.5 to 0.9 values of evaporative fraction as shown by Su (2002).

Main advantages of the SEBS include: (1) to reduce the uncertainty involved in surface temperature or meteorological variables by considering the limiting boundary condition to implement the energy budget equation; (2) instead of using a constant value, SEBS include modern approach to incorporate the roughness height for heat transfer; (3) characterizing actual surface heat fluxes without any prior information of extreme conditions; and (4) the comprehensive formulation considering the surface resistance related parameters. It is worth mentioning that SEBS has been broadly applied to several different ecosystem mainly by focusing on the coarse scale spatial resolution of 1 km information obtained from thermal band of MODIS data. Since the solution of turbulent heat fluxes involves relatively complex formulation that require several parameters both derived from the remote sensing information which may cause more or less inconsistencies in SEBS application

3.1.4 Uncertainties in Remote Sensing data and ET Retrieval Algorithms

Problems in Surface Temperature & Emissivity: Various remote sensing approaches that are used to derive surface temperature use Thermal Infrared (TIR) radiation data. For the estimation of surface temperature, the atmospheric and surface emissivity corrections will therefore affect the data quality provided by remote sensing. Two surface temperature correction methods, namely direct and indirect methods, could be applied. The direct method uses atmospheric sounding combined with the radiative transfer model; however, the indirect method uses only remote sensed observations. Typical uncertainties approximately in the range of 1–3 K

ICARDA
Science for resilient livelihoods in dry areas

RESEARCH
PROGRAM ON
Water, Land and
Ecosystems
CGIAR

happens due to atmospheric correction. Emissivity is the other critical component, which can lead to significant error. Both surface emissivity and directional infrared temperature are usually based on various spectral resolution which may help to reduce the errors to some extent and this is one of the most promising way to obtain such data (Byun et al., 2014).

Satellite Coverage Uncertainties: As satellites provides the several spatial resolution imageries which usually have the low temporal frequency, simultaneously acquiring the imagery of high spatial and temporal resolution is very difficult. TIR methods is biased towards the clear sky conditions due to the impediments created by clouds in obtaining continuous satellite imagery. In operation application this method can be impractical due to the larger time in obtaining the satellite imagery and ET estimation. This issue could be solved by coupling models and gap filling methods (Ershadi et al., 2013).

Errors in Solar Parameters Estimation: Individual parameters estimations of energy (Rn--G) caused uncertainties in the both long and short-wave components estimation and ignores diurnal variation and phase difference between each diurnal cycle of parameters. Furthermore, total Rn flux is only considered in SEB models, but there are no relative fractions for direct and diffuse radiation as well as no considerations for diffuse and direct radiation difference. Because of bulk use of vegetation, the impacts of increased diffuse radiation than direct radiation must be considered (Campos et al., 2013). A sufficient difference in ET measurement is highly expected if such differences are ignored in water use efficiency.

Land Surface Variables: Uncertainties need to be corrected in the radiance estimation which is caused atmosphere effects. Despite significance advances, for the accurate measurement of ET there is still needs to improve the accuracy of some remotely sensed land surface parameters e.g. LAI, VI, plant height and surface temperature, etc. The estimation of the aerodynamic resistance (ra) requires stability corrections, along with sufficient values for zero displacement level and roughness lengths. To recover the surface temperature the angular observation effect is more critical and prominent on heterogeneous surfaces as compared to homogenous well-watered and dense vegetative surfaces. Different radiation will be received when the sensor vision changes

from one angle to another due to the different type of vegetation and soil in field (Singh and Irmak, 2011; Sugita and Brutsaert, 1991)

Inconsistency of RS Models and Near-Surface Meteorological Variables: Different models are utilized for different characteristics of land surface. But still there is no universal model, which can be used worldwide, without any change or improvement to measure ET to form the satellite data, regardless of changes in earth characteristics in terrain and climate.

Frequently needed Meteorological data at near surface height or PBL height in most of ET models and are acquired, using spatial interpolation on local meteorological stations data, at a satellite pixel. Due to large differences in terrain and climate conditions in the area to be studies irregularly located meteorological stations and accuracy of interpolation methods must be improved.

3.2 Actual evapotranspiration databases

Many hydro-meteorological applications such as irrigation scheduling, crop water productivity estimation, allocation of water resource, and drought predictions require the accurate quantification of reliable ET estimation (Khan et al., 2018). However, due to the involvement of complexed land surfaces and environmental conditions, sensitive climate feedback, as well as their large unpredictability in both time and space usually cause extensive qualitative and quantitative inconsistencies in the ET quantification (Ghilain et al., 2011). Substantial effort has been made in the last one to two decades to generate multi-level regional to global scale ET datasets by gathering the information from recent advancements in satellite remote sensing technologies and conventional ground-based information (Ghilain et al., 2011). Although there are several available global actual ET products , the most generally available datasets with operational applications and larger coverage are MODerate resolution Imaging Spectroradiometer (MODIS) i.e., MOD16 AET (Mu et al., 2007) with eight-day, monthly and yearly temporal and 1 km spatial resolution, Global Land Evaporation and Amsterdam Model (GLEAM) 25 km daily AET products (Miralles et al., 2010), Wapor ET dataset (Blatchford et al., 2019) at 30m to 250 m spatial and monthly and annual temporal resolution, and Global Land Data Assimilation System (GLDAS) having 25 km AET

products at 3 hourly and monthly temporal resolution (Rodell et al., 2004). The further details of these ET products are provided below:

3.2.1 WaPOR

The Water Productivity through Open access of remotely sensed (WaPOR) derived data being published through the Food and Agriculture Organization of the United Nations (FAO-UN) (https://wapor.apps.fao.org/catalog/WAPOR_2/1), as a major output of the project: '*Using Remote Sensing in support of solutions to reduce agricultural water productivity gaps'*, funded by the Government of The Netherlands. The major aims of the WaPOR dataset is to provide "Free Access Water Productivity System ", for the countries such as Africa and the Middle East which are facing acute water crisis in recent years. The WaPOR database is a comprehensive database that provides information on biomass production (for food production) and evapotranspiration (for water consumption) for Africa and the Near East in near real time covering the period 1 January 2009 to date. The major products include, water productivity, biomass production, net primary productivity, precipitation, NDVI, land cover classification as well as evapotranspiration and its components.

As described in (Bastiaanssen, 2000), the method to calculate ET for the WaPOR product is based on the ETLook model which deals the E and T as separate components. This method utilizes the remote sensing as the primary input datasets which is forced through the Penman-Monteith (P-M) equation (Monteith, 1965). The P-M method employed frequently measured meteorological information such as air temperature, vapour pressure solar radiation, and wind speed for the estimation of total evaporation and transpiration over larger areas. The main concepts of the ETLook model lies in solving the two parallel Penman-Monteith equations as seen in Figure 1 below. The ETLook model framework treats two different approaches; first it coupled the soil with the subsoil or rootzone soil moisture content to derive the transpiration while the evaporation is estimated by coupling the soil moisture content available in the top soil surface. However, this model also deals with the interception to account for the amount of

rainfall which is intercepted by the leaves or use the energy to directly evaporate from the plant surface and not usually not available for the transpiration.

"The WaPOR portal delivers open access to three different spatial data layers related to land and water use for agricultural production and allows for direct data queries, time series analyses, area statistics and data download of key variables to estimate water and land productivity gaps in irrigated and rain fed agriculture". One of the most vital products of the WaPOR system is to provide the actual ET information, which is available at a spatial resolution of 250 m pixel size with s temporal resolution varying from an annual, monthly and 10-days for the 2009–2016 period using the ETLook algorithm (http://www.fao.org/in-action/remote-sensing-for-water-productivity/wapor/). There are not many studies have been published to evaluate these products over the Middle East and Africa since the public availability of WaPOR dataset (i.e., 2017), however, there is strong and urgent need to conduct such studies considering the large uncertainties of ET estimates over these dry environments. This would be a useful alternative to study the water productivity gaps as an alternative to the current methodologies.
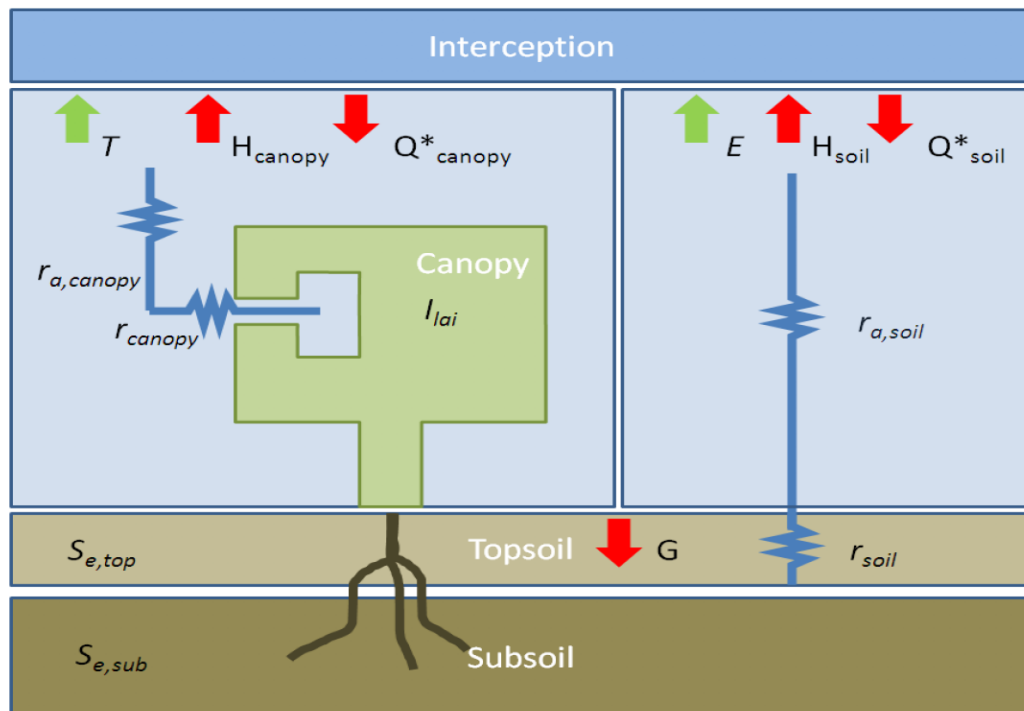

Figure 1: Schematic showing the partition of evaporation and transpiration in ETLook model

3.2.2 MOD16 Actual Evapotranspiration (AET) product

MOD16 is a land surface global terrestrial AET which was developed by Mu et al. (2007) through an improved remote sensing-based Penman-Monteith algorithm originally provided by Cleugh et al. (2007). The MOD16 global ET product considers the transpiration from the vegetation structure as well as represents all evaporation from soil and wet surfaces.

It is important to note that the original MOD16 algorithm was used to ignore the ground heat flux, intercepted evaporation from plant canopies and the night-time ET values and estimate actual ET for only daytime fluxes (Mu et al., 2007). The MOD16 algorithm was improved (Mu et al., 2011) further by "(i) the sum of day and night-time components of ET were incorporated to estimate the final daily ET product, (ii) vegetation cover fraction formulation in the model was simplified, (iii) ET calculation were updated by including specifically the ground heat flux especially for the tundra biome, (iv) applying an improved method to estimate stomatal conductance estimations were improved by applying the aerodynamic resistance and boundary layer resistance, (v) canopy water loss from the wet and dry surface was estimated separately, and (vi) saturated wet and moist surface were divided in order to incorporate potential and actual evaporation from the saturated and moist surface, respectively (Mu et al., 2013)."

MODIS albedo product (MCD43B2/MCD43B3), LAI/fPAR (MOD15A2), global 1-km^2 MODIS land cover (MOD12Q1) (Friedl et al., 2010) in conjunction with the and NASA's MERRA Global Modeling and Assimilation Office (GMAO) daily meteorological reanalysis dataset are the primary inputs used in the MOD16 algorithm (Mu et al., 2007). The standard outputs of the MOD16 algorithm include 8 days, monthly, and annual scale latent heat flux (LE), Potential LE, and PET (Kim et al., 2012) with spatial resolution of 500 m to 100 m and are available from 2000 to present (http://www.ntsg.umt.edu/project/mod16).

3.2.3 GLEAM Actual Evapotranspiration Product

GLEAM (www.gleam.eu) is a sophisticated land surface model that generate global actual ET product by using only satellite forcing data (Mastrocicco et al., 2010). The GLEAM ET datasets make a distinction between soil evaporation, open water evaporation, transpiration from short and tall vegetation, snow sublimation, and interception losses from various crop covers. Interception

loss is independently calculated based on The Gash analytical model using precipitation as forcing datasets is being considered in GLEAM to independently estimates the interception losses (Mastrocicco et al., 2010). While the P-T method (1972) is used to estimate the other remaining evaporation components (i.e. evaporation, sublimation, and transpiration). This is worth mentioning that unlike the P-M method, the P-T method does not incorporate parameterization of aerodynamic and stomatal resistance. Different independent satellites data are used as forcing inputs of GLEAM to generate global AET dataset with a spatial resolution of a quarter degree covering the period from January 1st, 1980 to December 31st, 2011 and are freely available at VU university Amsterdam Geoservices website (http://geoservices.falw.vu.nl) (Yang et al., 2015). The micrometeorological flux measurements at 43 FLUXNET global network covering various climatic and land surface conditions were used to validate the GLEAM ET product at regional to global scale (Miralles et al., 2010).

3.2.4 Global Land Data Assimilation System (GLDAS)

GLDAS (https://ldas.gsfc.nasa.gov/gldas/) data is produced by using the advanced and sophisticated land surface modelling and data assimilation methodologies which takes the combination of satellite and ground-based measurements to produce land surface states and an available field of fluxes (Rodell et al., 2004). GLDAS is running multiple land surface models Variable infiltration capacity (VIC) and (LSMs) such as Noah, Mosaic, Community land model (CLM). These LSMs models delivers the global fluxes in coarse and fine spatial (0.25°, 0.01°) and temporal (3-hourly and monthly) resolution by integrating a huge number of observational datasets. The NASA's Hydrology Data and Information Services Center (http://disc.sci.gsfc.nasa.gov/hydrology) exhaustively describe the information of different models and their forcing dataset.

3.3 Surface energy balance algorithm (SEBAL) for ET

The SEBAL model was selected to derive the evapotranspiration which has the distinguished capacity to provide ET at the high spatial resolution which is useful to map the crop water productivity across any basin with high accuracy. There are several developments made to this

model which has led its implementation in such a way that is effective, reproducible and reliable for the quantification of ET with higher accuracy, as discussed earlier in this report.

The SEBAL model has been applied for the ET quantification and extensively validated under several varying conditions across the globe in several countries (Awan et al., 2016; Bastiaanssen, 2000; Bastiaanssen et al., 1998; Singh et al., 2008; Timmermans et al., 2007). These studies compared their experimental results with the estimated fluxes from the SEBAL and confirm the robustness of the model formulation. The model has also been tested with remote sensing information from different satellites having a combination of high-temporal resolution such as Landsat7 ETM+/ASTER as well as high-spatial resolution such as NOAA AVHRR/MODIS to assess evapotranspiration rates at daily, monthly seasonal and annual scales with least ground-based weather information (Awan et al., 2016; Bastiaanssen, 2000).

3.3.1 Theory

SEBAL computes heat and water vapour transport for each pixel by solving the resistance for momentum with a complete radiation and energy balance model. Evapotranspiration is computed by means of instantaneous latent heat flux, λET, (W m^{-2}), and which is computed pixel-by-pixel basis for the time of satellite overpass as the residual of the surface energy balance equation:

$$\lambda ET = (Rn - G - H) \tag{7}$$

where Rn is net radiation (W m^{-2}), G is the soil heat flux (W m^{-2}), and H is the sensible heat flux (W m^{-2}). Net radiation is computed from the land surface radiation balance as:

$$Rn = (1 - \alpha)\,RSin + RLin - RLout - (1 - \varepsilon 0)RLin \tag{8}$$

where RS_{in} is the incoming short-wave solar radiation, RL_{in} and RL_{out} are incoming and outgoing long-wave radiation (W m^{-2}), ε_0 is the land surface emissivity, α is the surface short-wave albedo. These all parameters are calculated by the land surface parameterization schemes though implementing the standard algorithms.

Soil heat flux (G) is calculated by using the net radiation and a few other land surface physical parameters, such as surface temperature, albedo, and normalized difference vegetation index (NDVI) through an empirical relationship function defined by Bastiaanssen (2000):

$$G/Rn = Ts/\alpha(0.0038\alpha + 0.0074\alpha2)(1 - 0.98NDVI4) \qquad (9)$$

where Ts is surface temperature in K.

Sensible heat flux which is difficult to compute due to the interrelationship of surface roughness and temperature gradient. Bastiaanssen (2000) given the standard expression for sensible heat flux computation as following:

$$H = \rho C_p \frac{dT}{r_{ah}} \qquad (10)$$

Where ρ is the air density (kg m^{-3}) which is a function of atmospheric pressure, Cp is the dT is the near surface temperature difference (K), specific heat capacity of air ($\approx$1004 J kg^{-1} K^{-1}), r$_{ah}$ is the aerodynamic resistance to heat transport (s m^{-1}).

As described earlier, the SEBAL model introduce a linear relationship among the surface temperature Ts and dT which is iteratively calibrated on the basis of information from two extreme boundary conditions which are pre-located within the image itself whereas the dT values can be iteratively computed using the known sensible heat flux for both extreme conditions as expressed in equation (1).

The coefficients "a" and "b" in Equation (1) can be effectively assessed, once the surface-air temperature differences for both the extreme condition (i.e., hot and cold anchor pixels) is determined. These coefficients "a" and "b", are then utilized in an iterative setup in the model to develop a linear gradient of the surface-air temperature difference dT for each pixel of the image by using land surface temperature in Equation (1). In SEBAL model, the hot pixel is chosen from an image pixel which is representing an area with least vegetation or displays high surface temperature, while the cold pixel is generally choose from a pixel located in well-watered crop conditions assuming no stress conditions. With the user defined extreme anchor pixels, the sensible heat flux is usually calculated iteratively with corrected roughness length for the stability, while this procedure also required an extrapolation of wind speed from ground level to a height of about

100 to 200 m. Usually, the identification of wet pixels are easily spotted over an area of well-watered surfaces or over a relatively large, calm water surface, whereas recognizing the dry pixels is the foremost vital perspective in SEBAL. The instantaneous latent heat flux, λET, which is computed as the residual term of the energy budget is further used to estimate the instantaneous evaporative fraction Λ:

$$\Lambda = \frac{\lambda ET}{\lambda ET + H} = \frac{\lambda ET}{R_n - G_0} \tag{11}$$

When the atmospheric moisture conditions are in equilibrium with the soil moisture conditions, the instantaneous evaporative fraction Λ expresses the ratio of the actual to the crop evaporative demand. As demonstrated by the several previous studies (Singh et al., 2008; Teixeira et al., 2009) that the Λ values are almost remains constant within daytime hours, thus allowing the use of as a temporal integration of ET over larger timescale. For timescales of 1 day or longer, G can be ignored and the net available energy (Rn − G) reduces to the net radiation (Rn). At daily timescales, ET_{24} (mm d^{-1}) can be computed as:

$$ET_{24} = \frac{86400 \times 10^3}{\lambda \rho_w} \Lambda R_{n24} \tag{12}$$

where: R_{n24} (W m^{-2}) is the 24 h averaged net radiation, λ (J kg^{-1}) is the latent heat of vaporization, and ρ_w (kg m^{-3}) is the density of water. The monthly and seasonal ET values were estimated by linear interpolating the daily ET values for the period in between two consecutive images.

3.3.2 Image Acquisition

The key parameters in SEBAL formulation, includes albedo, Land Surface temperature (LST) and vegetation index, for portioning the available energy between vegetation and soil. The Moderate-resolution Imaging Spectroradiometer (MODIS) is one of the complex programs which use the sensors of two satellites (Aqua and Terra) to give a detailed series of global observations in infrared and visible spectrum of ocean, land and atmosphere of earth. Terra earth observation system (EOS) was launched in 1999 and it passes around 10:30 A.M. over the region to be studies. The MODIS is available and downloaded in different versions and the latest version 5 (V005) from the NASSA online web portal (https://reverb.echo.nasa.gov/reverb) which is available from 2014

and used in this study of the measurement of ETa globally. SEBAL model requires the MODIS imagery including the surface reflectance (SF), surface emissivity (EMM), LST, and vegetation indices (VI). All data sets have 8 days temporal resolution except LST data, because during the short time period the land surface properties does not change, which instantaneously collected with daily time period at overpass time of satellite.

To provide the Normalized Difference Vegetation Index (NDVI), Vegetation index (VI) products is scaled by multiplying with 0.0001. The undisputed key indicator of ET flux is NDVI (Allen et al., 2011; Liaqat et al., 2014; Su, 2002). To create the 8 days 250 NDVI layers the two 16-day data sets of NDVI (MYD13and MOD13) starts from day 1 and day 9 were used. Therefore, for the period 2014-2019, the other products of MODIS were obtained and reprojected to 8-day scale. The average surface emissivity was estimated by taking average of Em_31 (from band 31) and Em_32 (from band 32) and then scaled with minimum Em up to +0.49 by 0.002. Also surface reflectance (bands 1–7) were computed from the products of the daily land surface reflectance and then scaled by 0.0001. The surface albedo was computed using the Liang's method from the seven surface reflectance bands. To cover the period from 2014 to 2019 over the Nile data area, total 638 sets of MODIS images was reprojected.

3.3.3 Meteorological Data

GLDAS (https://ldas.gsfc.nasa.gov/gldas/) data is produced by using the advanced and sophisticated land surface modelling and data assimilation methodologies which takes the combination of satellite and ground-based measurements to produce land surface states and an available field of fluxes (Rodell et al., 2004). GLDAS is running multiple land surface models Variable infiltration capacity (VIC) and (LSMs) such as Noah, Mosaic, Community land model (CLM). These LSMs models delivers the global fluxes in coarse and fine spatial (0.25°, 0.01°) and temporal (3-hourly and monthly) resolution by integrating a huge number of observational datasets. The NASA's Hydrology Data and Information Services Center (http://disc.sci.gsfc.nasa.gov/hydrology) exhaustively describe the information of different models and their forcing dataset. The GLDAS data simulated from the Noah 2.7.1 model contains a series of land surface parameters at a spatial resolution of 0.25º with 3-hour time step information. To

force the SEBAL algorithm, meteorological variables including specific humidity ($kgkg^{-1}$), wind speed (ms^{-1}), pressure (Pa), downward longwave and incident shortwave radiation (Wm^{-2}) were extracted from GLDAS (Rodell et al., 2004).

3.3.4 Validation of ET

SEBAL first estimates the instantaneous energy fluxes retrieved at sensor overpass times and then latter it is converted to diurnal values of energy fluxes which are practically more useful. Thus, the systematic model biases in flux components were analysed by comparing them with ground-based flux tower measurements. To achieve this, *in situ* flux tower measurements obtained during 10:30 am to 12:00 pm were averaged in the time domain to obtain the average fluxes around sensor overpass times. This is because MODIS sensors onboard Terra satellite passed over the study area mostly between 11:00 am to 12 pm local time. To determine the error and evaluate the performances of the SEBAL model in terms of surface energy flux, ground based observations were compared with estimated flux measurements before further forcing for diurnal scale ET calculations at both study sites, which had different vegetation characteristics. Agreement between the estimated and measured results was assessed in terms of bias, RMSE, and coefficient of determination (R^2), where $0 < R^2 \leq 1.0$, with greater R^2 values specifying better model agreement. The RMSE is a synthetic indicator of absolute model uncertainty and represents a measure of overall, or mean deviation between estimated and measured variables.

$$R^2 = \frac{n\left(\sum E \cdot O\right) - \left(\sum E\right)\left(\sum O\right)}{\sqrt{\left[n\sum E^2 - \left(\sum E\right)^2\right]\left[n\sum O^2 - \left(\sum O\right)^2\right]}}$$

(13)

$$BIAS = \frac{1}{n}\sum\left(E - O\right)$$

(14)

$$RMSE = \sqrt{\frac{1}{n}\sum_{i=1}^{n}\left(E - O\right)^2}$$

(15)

where E and O represent the estimated and observed (measured) variables, respectively, and n is the number of samples.

3.3.5 Results

For the validation and accuracy assessment of models we compared estimates with observations by extracting pixel values of spatially estimated evapotranspiration from SEBAL corresponding to the geographical locations of *in situ* flux tower. The graphical representation of statistical results shown in Figure 2 reveals that SEBAL estimations were reasonably well correlated with flux tower ETa, yielding high coefficient of determinations (R^2) of 0.87 with improved slope values that are close to 1:1 while RMSE values of 0.49 mm/day and bias of 0.13 mm/day.
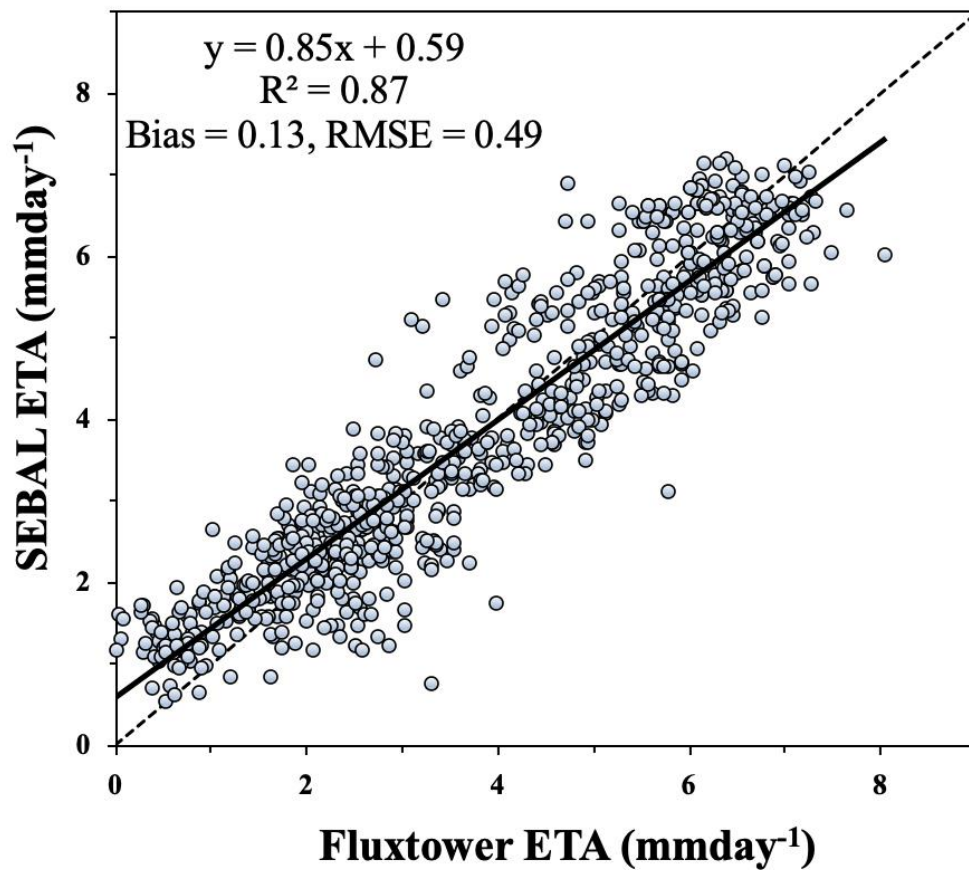
Figure 2: The accuracy comparison between SEBAL estimated and flux tower measured actual evapotranspiration (ETa)

These results agree with the previous findings (Awan et al., 2016; Bastiaanssen, 2000). However, this small difference is acceptable, considering the uncertainty embedded in surface measurements, as well as the scale difference between the MODIS 1 km pixel size and point scale meteorological measurements. The bias error was determined by subtracting the ETA of flux tower from the SEBS ETa. When the direction of the error was considered, the results showed that the SEBAL algorithm slightly overestimated the daily ETa respectively.

The daily ETa values estimated from the SEBAL were scaled up to monthly values for the year of 2018. The monthly variations in ETa for the entire Nile delta shown in Figure 3 below. In general, the monthly ETa appeared larger during the period of May to August, with mean minimum and maximum values of 33 mm and 232 mm, while during December and July minimum and maximum values of 9 mm and 87 mm observed, respectively. From hydrometeorological perspective, the high magnitude ETa values in these hot months are attributed to several factors such as high atmospheric water demands, increased irrigation for replenishment of soil moisture, and precipitation which ensured soil moisture at optimal conditions. The highest monthly ETa values are in July and August month, in which ETa values reaches upto 300 mm approximately all over the Nile delta region. In general, the highest average monthly values of ETa has been observed on north side of the Nile delta region.

Figure 4 presents, the annual variability of the SEBAL estimated ETa for entire area. The variation in annual ETa were relatively small, however in general the highest average annual values of ETa has been observed on north side of the Nile delta region, as represented in Figure 4. The mean yearly ETa values estimated by SEBAL were varied from 991 to 1036 mm / year for the entire study region, with a standard deviation value of approximately 322 to 345 mm /year during the period of 2014 to 2019. Frequency histogram of annual ETa demonstrating spatial variability with mean and standard deviation values has been shown in Figure 5. Histrogram for average annual ETa shows that the maximum and minimum annual mean ETa are 991 ($\pm$ 322) mm/ year and 1036 ($\pm$ 336) mm/ year in 2017 and 2016, respectively, which shows relatively small variation of annual ETa.
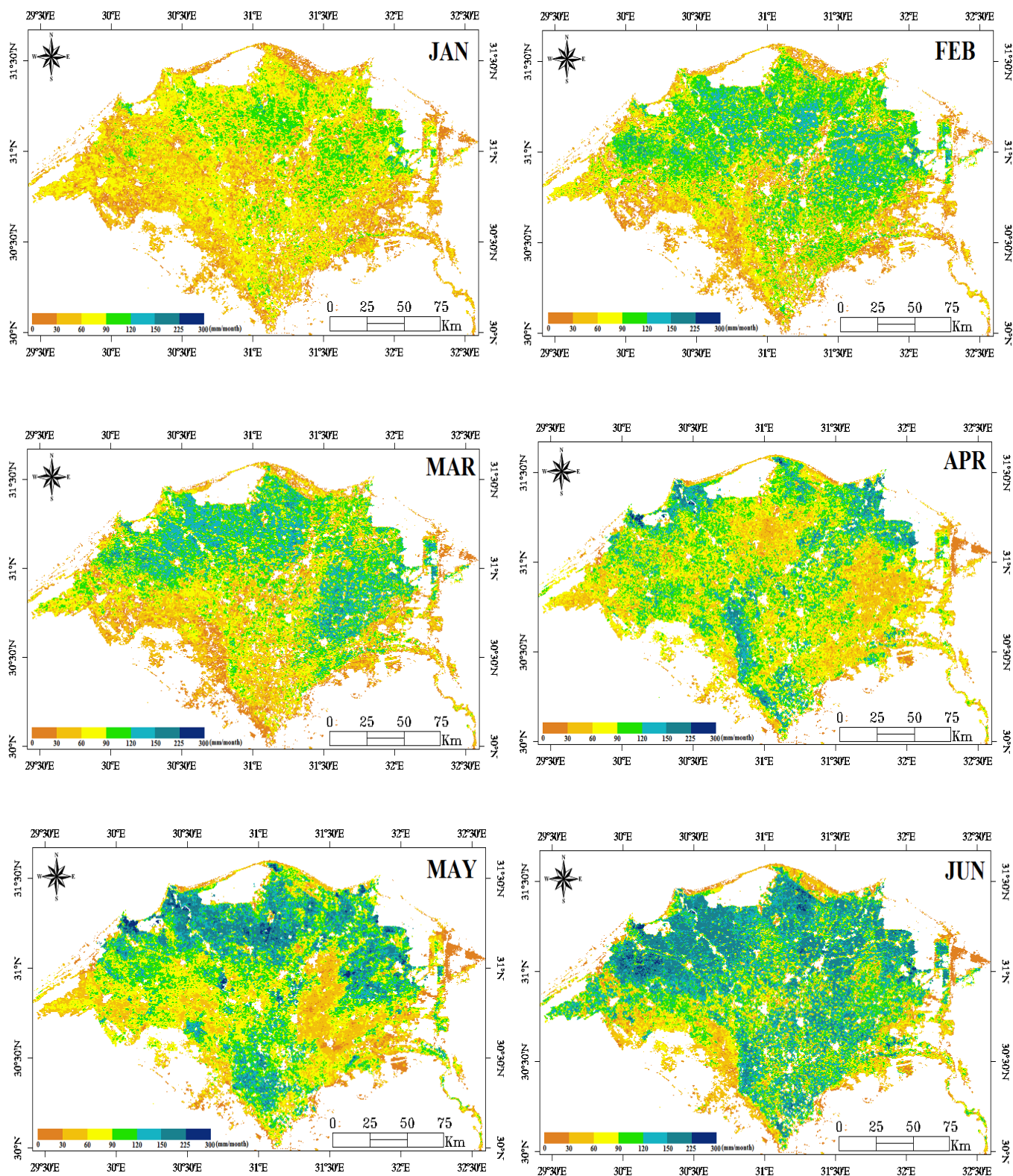
Figure 3: Spatial variations in monthly ETa estimated by the SEBAL approach (cont'd)
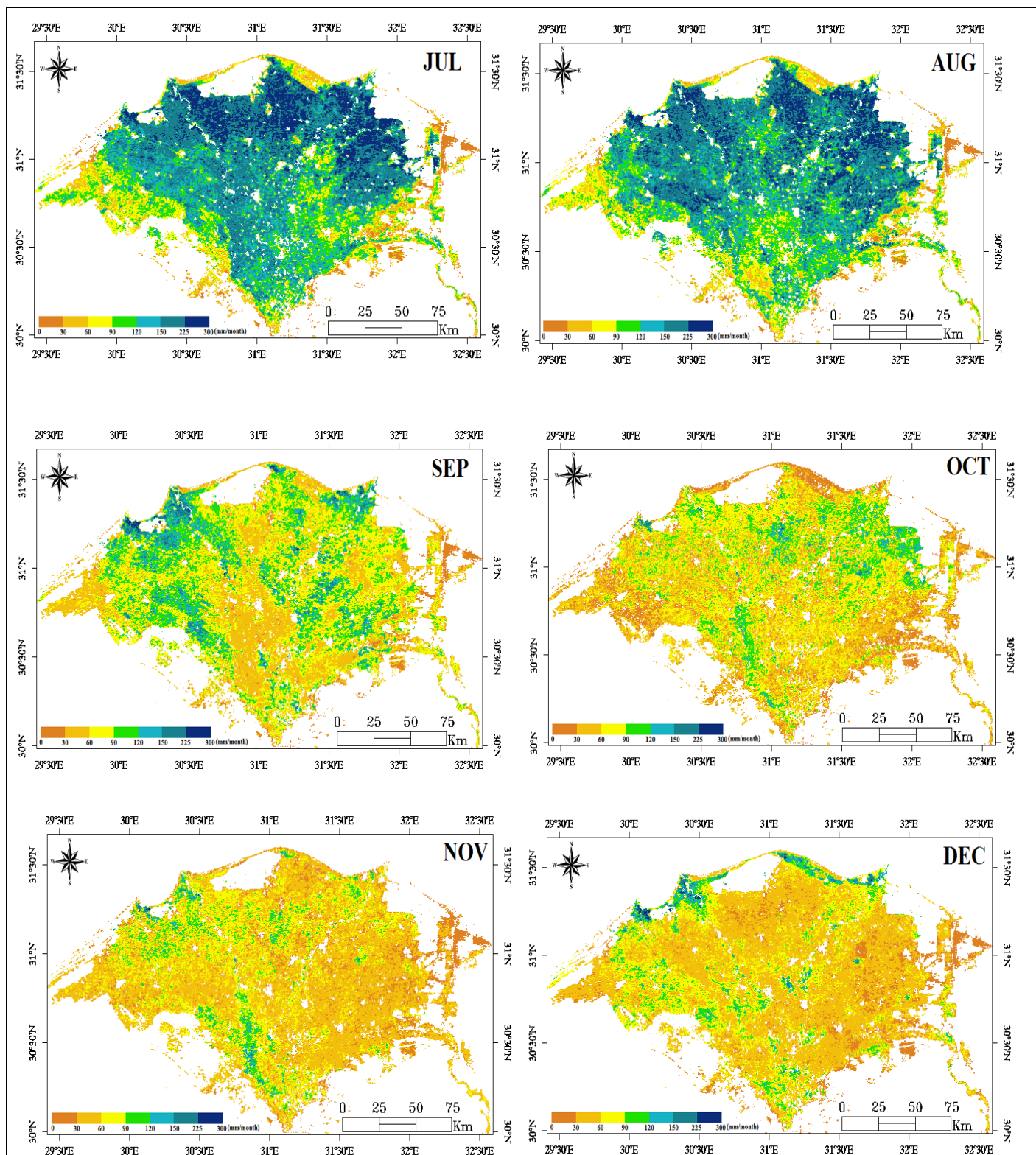
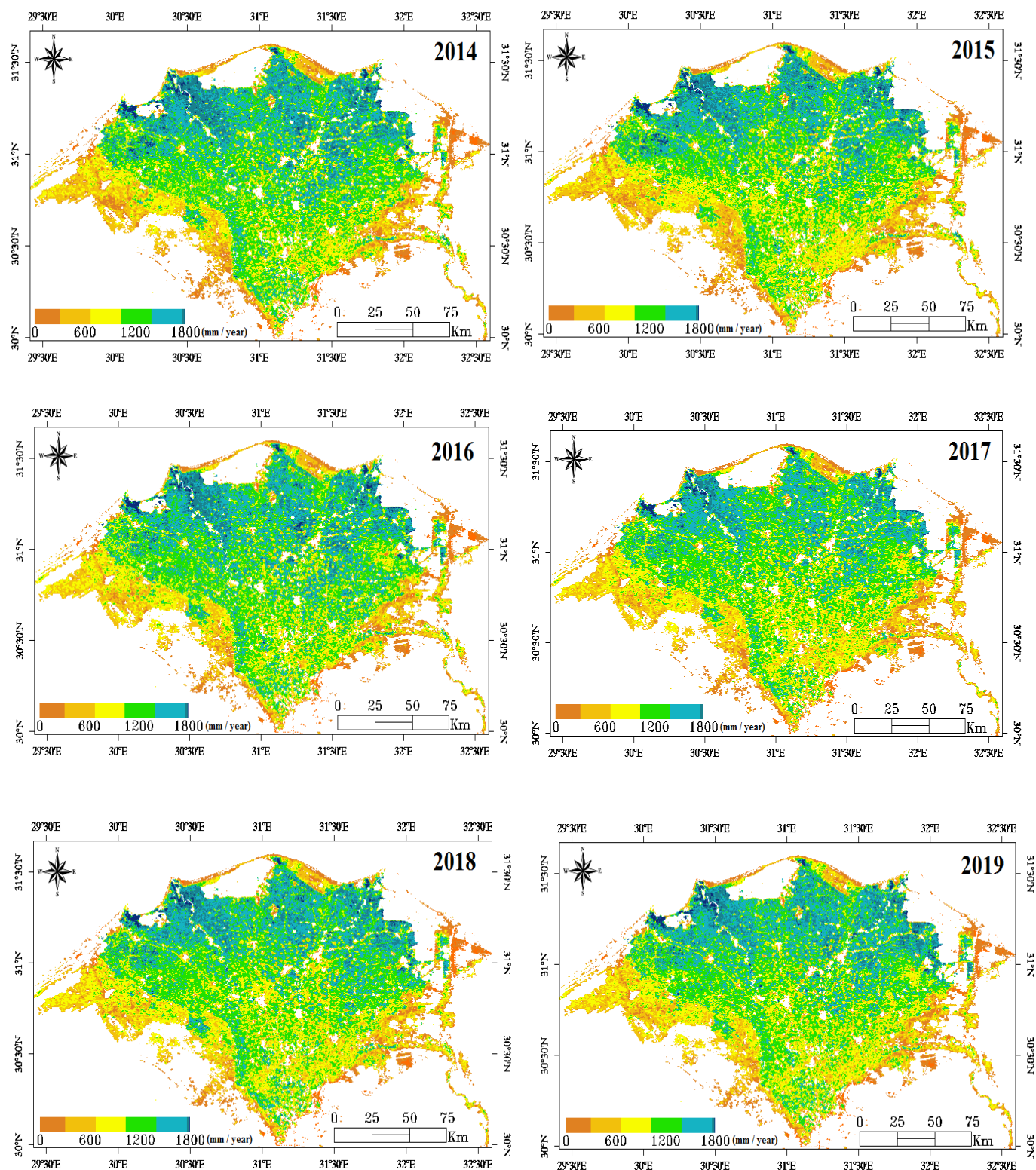Figure 3: Spatial variations in monthly ETa estimated by the SEBAL approach

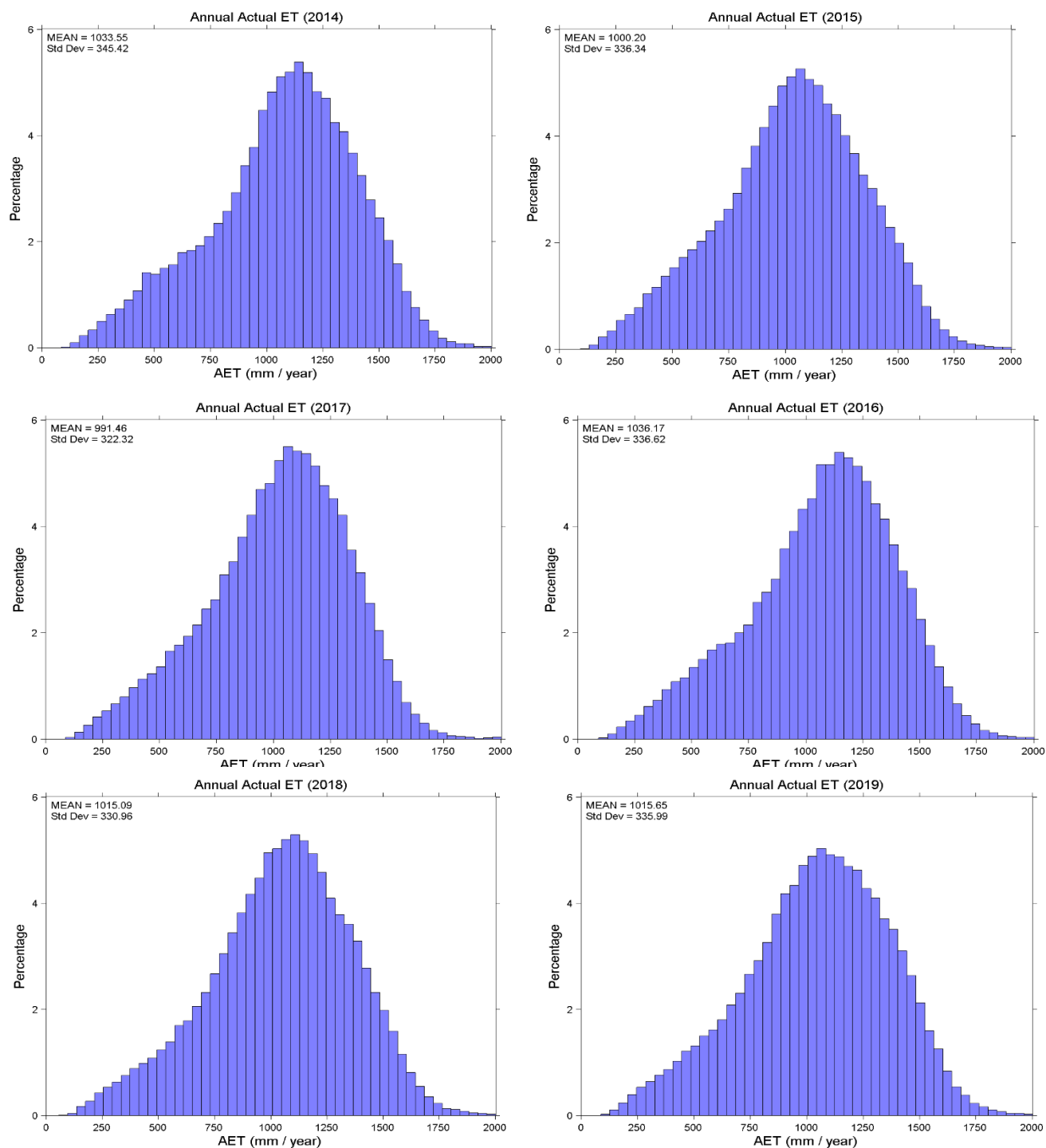Figure 4: Spatial variations in annual ETa estimated by the SEBAL approach

Figure 5: Frequency histogram of annual ETa demonstrating spatial variability with mean and standard deviation values

3.4 Biomass estimates by remote sensing

Crop biomass is one of the key indicators not only in crop condition monitoring, but also in crop production estimation. With the development of technology, it is feasible to estimate crop biomass at large scales with remote sensing.

3.4.1 Theory

One of the key indicators of agro-ecosystems, is known as above-ground biomass (AGB), which is usually used as a key component in estimating water use efficiency as well as predicting crop production (Jin et al., 2018; Nair et al., 2013). Accurate, rapid and economical quantification of AGB is of great significance as it always remains one of the basic factor to research agro-ecosystem processes (Walter et al., 2018), to assess the performance of agricultural practices , and to estimate global market risk (Basso et al., 2016). The main data source for large-area AGB estimation is currently utilized from various remote sensing sources (Basso et al., 2016) which is an significant data source that could be widely used to quantify the field to regional scale AGB.

Among several developed methods to quantify AGB by means of satellite remote sensing data, whereas the empirical relationships between NDVI and AGB is developed and this method is the most common among the hydrologic community. The common problem in various methods which used NDVI and AGB empirical or statistical relationships is that those methods have the correlation coefficients values ranging from moderate to low due to their strong empirical character (Jin et al., 2018; Walter et al., 2018). To collect AGB in the field, most of those empirical approaches require extensive field measurement programs, which is not only expensive or laborious but also practically difficult to consider at large regional scale. There is an extensive literature which represents that the biomass production model proposed by Monteith (1972) based on leaf development and solar radiation has potential to acquire AGB at large scale with reasonably high accuracy and this method can be used in combination with the satellite imagery.

The SEBAL estimated actual ET and satellite derived NDVI values were used to produce the ABG, for each pixel of the satellite images. The fraction of absorbed photosynthetically active radiation (fPAR) = absorbed PAR (APAR)/total PAR (PAR), the SEBAL estimated evaporative fraction (Λ) and constant light use efficiency (LUE) values were used to achieve the purpose. The

NDVI image of the area was used to estimate the fPAR as shown in Equation (16) (Gobbo et al., 2019):

$$fPAR = -0.161 + 1.257 \times NDVI \tag{16}$$

$$ABG = LUE \times \Lambda \times fPAR \times 0.84 \tag{17}$$

An average value of light use efficiency factor was set at 4 g/MJ (Vermote et al., 1997). The total above groundmass (ABG) production applying multiplying the ABG values obtained in equation (18) to 0.77 (Gobbo et al., 2019).

3.4.2 Results of estimated biomass

The above ground biomass (ABG) was estimated by using the equation and variability in ABG on yearly basis has been presenting in the Figure 6 below. Spatial variation of ABG values ranges from the 0 to 40 t/ha for the entire area while variations among yearly biomass estimations were relatively large but the variations capturing at the small field scale were relatively low. This is because of the low-resolution image used from the MODIS. In order to get field scale field scale productivity, the high-resolution image should be utilized.

Moreover, the biomass generally showed an increasing trend from south to the north in the region which is probably due to the high proximity of available water in those areas. Average biomass for the area was ~ 15 (T/ha) with a variation of ~7 (T/ha), while the spatial mapping showed the evidence that biomass production was decreased with increase in number of years such that lowest biomass production was observed during the year of 2017.

Maps shows that biomass production is highest at north side of the Nile delta region. There is relatively small variation in biomass production annually. The maximum and minimum annual biomass production in Nile delta region for period 2014-2019 was 8 (T/ha) to 23 (T/ha), which also suggest that there is need to incorporate the advanced interventions in the regions where biomass production is less than the average values in order to increase the water productivity and utilize the available water resources in best possible manner.
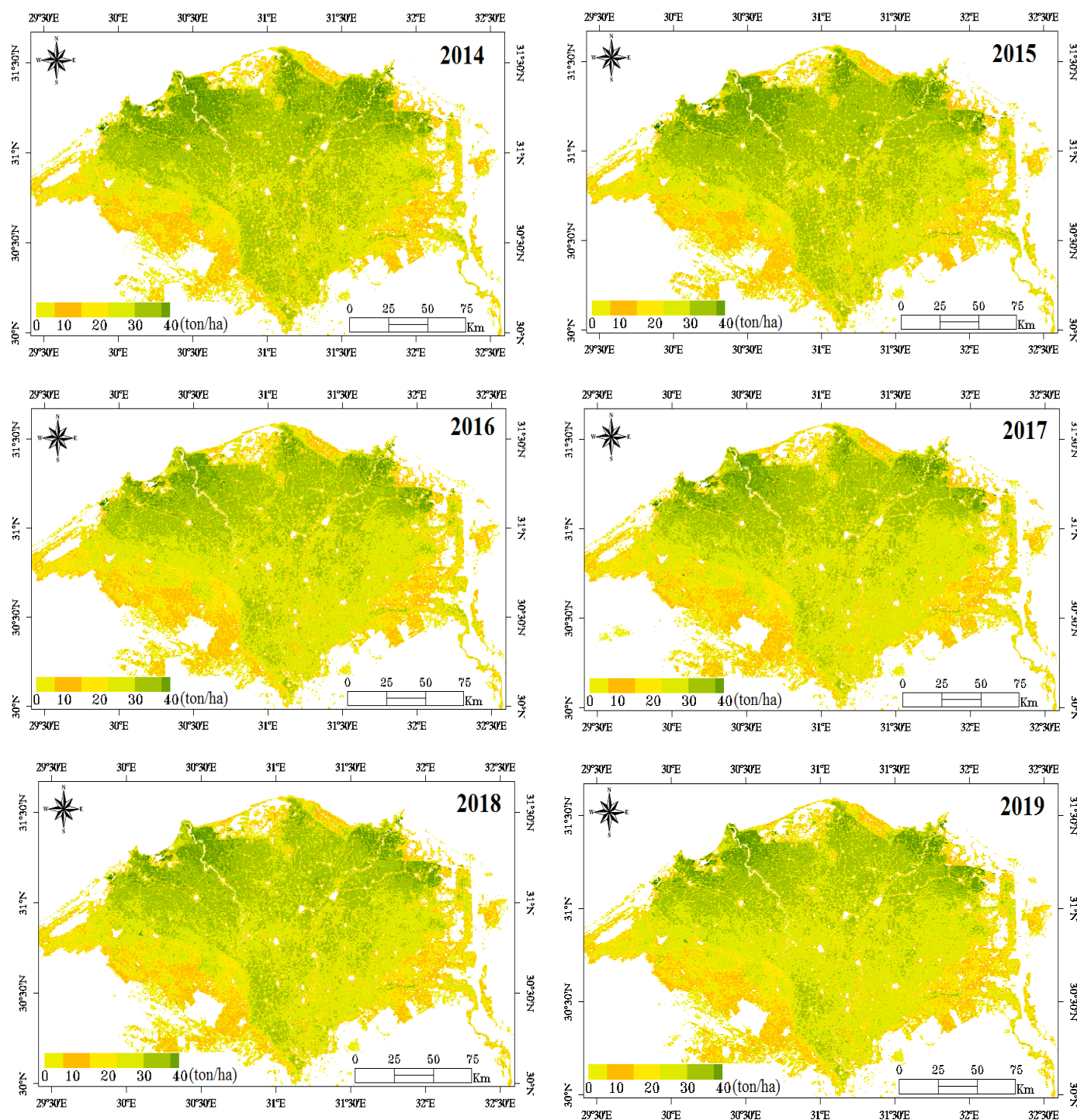
Figure 6: Spatial variations in above ground biomass (ABG) covering the period 2014-2019

3.5 Water productivity estimates by remote sensing

For evaluating the agriculture water management, the key indicator to relate crop production to water use is water productivity. Worldwide largest consumer of fresh water in the world is irrigation, which facing the huge pressure due to food demand, climate change, water use competition within sectors. Water productivity (WP) signifies the benefits (in $ / ha), or fresh crops (in kg / ha) produced per unit of water consumed or applied (in kg / m3). As actual evapotranspiration (ET) also include non-irrigation water such as soil moisture changes, capillary rise and rainfall, therefore it is recommended to analyse the CWP in terms actual ET (Gobbo et al., 2019; Grosso et al., 2018). Sustainable agriculture needs to increase water productivity by with water, producing more food. Remote sensing-aided water productivity evaluation helps to evaluate the improvement potential and pinpoint the bright or hot spots.

Agricultural water productivity is the economic value of production or physical mass production (e.g., grain yield, biomass) to water delivered or used for the production (Molden, 1997). How the system converts water into services and goods can be measured by WP (equation 18). Water productivity (WP) can be derived by using the following equation:

$$WP \ (kg/m^3) = \frac{output \ from \ water \ use(kg/m^2)}{water \ input \ (m^3/m^2)} \tag{18}$$

Output derived from water use including products, e.g., crop yield, biomass, fish, and livestock production which are all can be measure in economic values (e.g., dollars) or can be measure in unit of kilogram. Water input can be irrigation, available water, net inflow, gross inflow and actual evapotranspiration. In this study the crop productivity use as nominator and use of water per unit area as denominator, which are estimated by remote sensing approach using ground information.

The water productivity for the Nile delta was estimated by using the above ground biomass and actual evapotranspiration products and the results of WP for the period of 2014-2019 has been represented in the Figure 7 below. Spatial variation of WP values ranges from the 0 to 4 kg/m^3 for the entire area while variations among yearly WP estimations were relatively large. It is also worthy to note that field scale variations could not be captured due to the low-resolution images used from the MODIS. The high-resolution image should be utilized to obtain the field scale water productivity.
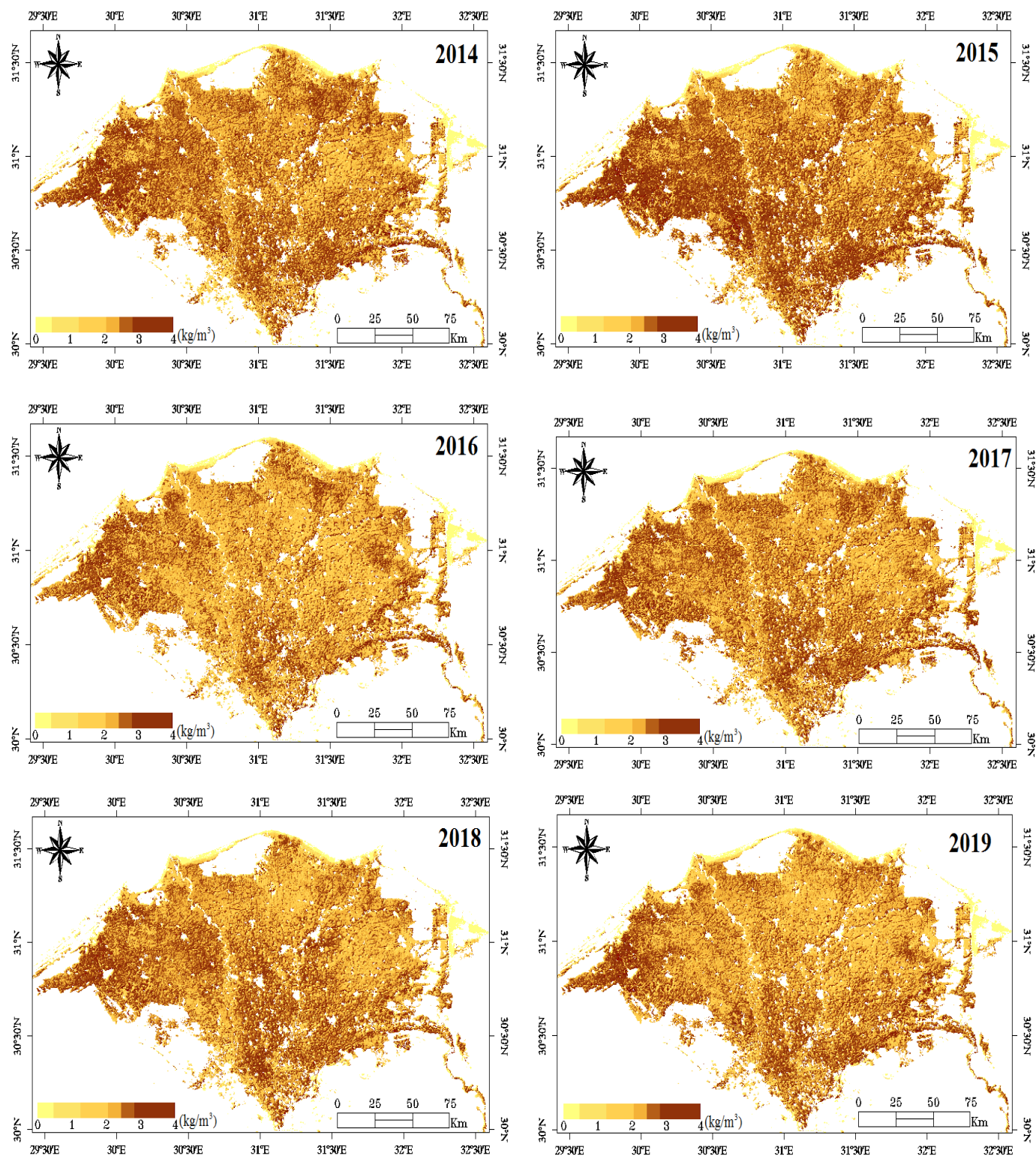
Figure 7: Spatial variations in water productivity covering the period 2014-2019

Moreover, the WP generally showed an increasing trend from east to the west in the region (Figure 7) which is probably due to the high proximity of available water close to the sea. Average WP for the area was ~ 1.62 (kg/m^3) with a variation by means of standard deviation ~0.5 (kg/m^3) while the spatial mapping showed the evidence that WP was decreased with increase in number of years such that lowest WP was observed during the year of 2016 (Figure 8). The variability by the histogram values provided below shows that water productivity in the region mostly positioned from 1 to 2.5 kg /m^3 which is good indicator of utilization of available water resources. However, the spatial mapping results suggest that there is significant scope of increasing water productivity in the areas with its minimum values < 1 kg /m^3 without increasing the allocation of water and/or cropland resources in order to feed the expanding population in the coming years.
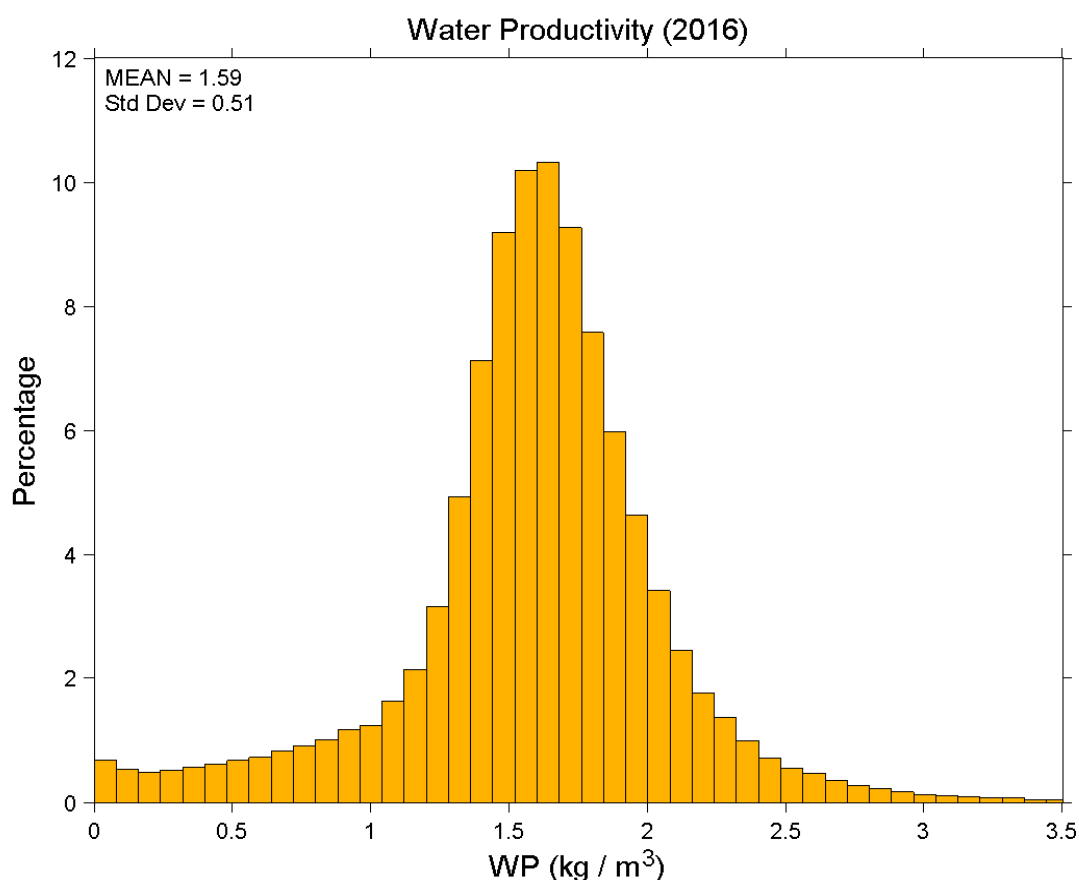

Figure 8: Frequency histogram of water productivity for the year 2016 demonstrating spatial variability with mean and standard deviation values

3.6 References

Ahmad, M.-u.-D., Bastiaanssen, W.M. and Feddes, R., 2005. A new technique to estimate net groundwater use across large irrigated areas by combining remote sensing and water balance approaches, Rechna Doab, Pakistan. Hydrogeol J, 13(5): 653-664.

Allen, R. et al., 2011. Satellite-based ET estimation in agriculture using SEBAL and METRIC. Hydrological Processes, 25(26): 4011-4027.

Allen, R.G. et al., 2013. Automated Calibration of the METRIC-Landsat Evapotranspiration Process. JAWRA Journal of the American Water Resources Association, 49(3): 563-576.

Allen, R.G., Pereira, L.S., Raes, D. and Smith, M., 1998. Crop evapotranspiration-Guidelines for computing crop water requirements-FAO Irrigation and drainage paper 56. FAO, Rome, 300: 6541.

Allen, R.G., Tasumi, M. and Trezza, R., 2007. Satellite-based energy balance for mapping evapotranspiration with internalized calibration (METRIC)—Model. Journal of irrigation and drainage engineering, 133(4): 380-394.

Awan, U.K., Anwar, A., Ahmad, W. and Hafeez, M., 2016. A methodology to estimate equity of canal water and groundwater use at different spatial and temporal scales: a geo-informatics approach. Environmental Earth Sciences, 75(5): 1-13.

Awan, U.K. and Ismaeel, A., 2014. A new technique to map groundwater recharge in irrigated areas using a SWAT model under changing climate. Journal of Hydrology, 519: 1368-1382.

Basso, B. et al., 2016. Environmental and economic benefits of variable rate nitrogen fertilization in a nitrate vulnerable zone. Science of the total environment, 545: 227-235.

Bastiaanssen, W., 2000. SEBAL-based sensible and latent heat fluxes in the irrigated Gediz Basin, Turkey. Journal of hydrology, 229(1): 87-100.

Bastiaanssen, W., Menenti, M., Feddes, R. and Holtslag, A., 1998. A remote sensing surface energy balance algorithm for land (SEBAL). 1. Formulation. Journal of hydrology, 212: 198-212.

Blatchford, M.L., Mannaerts, C.M., Zeng, Y., Nouri, H. and Karimi, P., 2019. Status of accuracy in remotely sensed and in-situ agricultural water productivity estimates: A review. Remote Sensing of Environment, 234: 111413.

Boegh, E. et al., 2009. Remote sensing based evapotranspiration and runoff modeling of agricultural, forest and urban flux sites in Denmark: From field to macro-scale. Journal of Hydrology, 377(3–4): 300-316.

Brutsaert, W.H., 1982. Evaporation into the Atmosphere: Theory, history, and applications. Reidel, Dordrecht, Holland.

Byun, K., Liaqat, U.W. and Choi, M., 2014. Dual-model approaches for evapotranspiration analyses over homo-and heterogeneous land surface conditions. Agricultural and Forest Meteorology, 197: 169-187.

Campos, I., Villodre, J., Carrara, A. and Calera, A., 2013. Remote sensing-based soil water balance to estimate Mediterranean holm oak savanna (dehesa) evapotranspiration under water stress conditions. Journal of Hydrology, 494: 1-9.

Choi, M., Kim, T.W., Park, M. and Kim, S.J., 2011. Evapotranspiration estimation using the Landsat-5 Thematic Mapper image over the Gyungan watershed in Korea. International Journal of Remote Sensing, 32(15): 4327-4341.

Ershadi, A., McCabe, M., Evans, J., Chaney, N. and Wood, E., 2014a. Multi-site evaluation of terrestrial evaporation models using FLUXNET data. Agricultural and Forest Meteorology, 187: 46-61.

Ershadi, A., McCabe, M.F., Evans, J.P., Chaney, N.W. and Wood, E.F., 2014b. Multi-site evaluation of terrestrial evaporation models using FLUXNET data. Agricultural and Forest Meteorology, 187: 46-61.

Ershadi, A., McCabe, M.F., Evans, J.P. and Walker, J.P., 2013. Effects of spatial aggregation on the multi-scale estimation of evapotranspiration. Remote Sensing of Environment, 131: 51-62.

Fisher, J.B., Tu, K.P. and Baldocchi, D.D., 2008. Global estimates of the land–atmosphere water flux based on monthly AVHRR and ISLSCP-II data, validated at 16 FLUXNET sites. Remote Sensing of Environment, 112(3): 901-919.

Ghilain, N., Arboleda, A. and Gellens-Meulenberghs, F., 2011. Evapotranspiration modelling at large scale using near-real time MSG SEVIRI derived data. Hydrology & Earth System Sciences, 15(3).

Gobbo, S. et al., 2019. Integrating SEBAL with in-Field Crop Water Status Measurement for Precision Irrigation Applications—A Case Study. Remote Sensing, 11(17): 2069.

Gowda, P.H. et al., 2008. ET mapping for agricultural water management: present status and challenges. Irrigation science, 26(3): 223-237.

Gowda, P.H. et al., 2013. Deriving hourly evapotranspiration rates with SEBS: A lysimetric evaluation. Vadose Zone Journal, 12(3).

Grosso, C. et al., 2018. Mapping maize evapotranspiration at field scale using SEBAL: A comparison with the FAO method and soil-plant model simulations. Remote Sensing, 10(9): 1452.

Hwang, K. and Choi, M., 2013. Seasonal trends of satellite-based evapotranspiration algorithms over a complex ecosystem in East Asia. Remote Sensing of Environment, 137: 244-263.

Jin, X. et al., 2018. Estimation of water productivity in winter wheat using the AquaCrop model with field hyperspectral data. Precision Agriculture, 19(1): 1-17.

Kalma, J.D., McVicar, T.R. and McCabe, M.F., 2008. Estimating land surface evaporation: A review of methods using remotely sensed surface temperature data. Surveys in Geophysics, 29(4-5): 421-469.

Khan, M.S., Liaqat, U.W., Baik, J. and Choi, M., 2018. Stand-alone uncertainty characterization of GLEAM, GLDAS and MOD16 evapotranspiration products using an extended triple collocation approach. Agricultural and Forest Meteorology, 252: 256-268.

Kim, H.W., Hwang, K., Mu, Q., Lee, S.O. and Choi, M., 2012. Validation of MODIS 16 global terrestrial evapotranspiration products in various climates and land cover types in Asia. KSCE Journal of Civil Engineering, 16(2): 229-238.

Li, S.-G. et al., 2006. Energy partitioning and its biophysical controls above a grazing steppe in central Mongolia. Agricultural and Forest Meteorology, 137(1): 89-106.

Li, Z.-L. et al., 2009. A review of current methodologies for regional evapotranspiration estimation from remotely sensed data. Sensors, 9(5): 3801-3853.

Liaqat, U.W., Awan, U.K., McCabe, M.F. and Choi, M., 2016. A geo-informatics approach for estimating water resources management components and their interrelationships. Agricultural Water Management, 178: 89-105.

Liaqat, U.W. and Choi, M., 2015a. Surface energy fluxes in the Northeast Asia ecosystem: SEBS and METRIC models using Landsat satellite images. Agricultural and Forest Meteorology, 214–215: 60-79.

Liaqat, U.W. and Choi, M., 2015b. Surface energy fluxes in the Northeast Asia ecosystem: SEBS and METRIC models using Landsat satellite images. Agricultural and Forest Meteorology, 214: 60-79.

Liaqat, U.W., Choi, M. and Awan, U.K., 2014. Spatio-temporal distribution of actual evapotranspiration in the Indus Basin Irrigation System. Hydrological Processes, doi: 10.1002/hyp.10401.

Liou, Y.-A. and Kar, S.K., 2014. Evapotranspiration Estimation with Remote Sensing and Various Surface Energy Balance Algorithms—A Review. Energies, 7(5): 2821-2849.

Mastrocicco, M., Colombani, N., Salemi, E. and Castaldelli, G., 2010. Numerical assessment of effective evapotranspiration from maize plots to estimate groundwater recharge in lowlands. Agricultural Water Management, 97(9): 1389-1398.

McCabe, M. et al., 2011. Multisensor Global Retrievals of Evapotranspiration for Climate Studies Using the Surface Energy Budget System, Land Remote Sensing and Global Environmental Change. Springer, pp. 747-778.

Miralles, D.G., Gash, J.H., Holmes, T.R., de Jeu, R.A. and Dolman, A., 2010. Global canopy interception from satellite observations. Journal of Geophysical Research: Atmospheres, 115(D16).

Molden, D., 1997. Accounting for water use and productivity. Iwmi.

Mu, Q., Heinsch, F.A., Zhao, M. and Running, S.W., 2007. Development of a global evapotranspiration algorithm based on MODIS and global meteorology data. Remote sensing of Environment, 111(4): 519-536.

Mu, Q., Zhao, M. and Running, S.W., 2011. Improvements to a MODIS global terrestrial evapotranspiration algorithm. Remote sensing of environment, 115(8): 1781-1800.

Nair, S., Johnson, J. and Wang, C., 2013. Efficiency of irrigation water use: a review from the perspectives of multiple disciplines. Agronomy Journal, 105(2): 351-363.

Rodell, M. et al., 2004. The global land data assimilation system. Bulletin of the American Meteorological Society, 85(3): 381-394.

Santos, C., Lorite, I., Tasumi, M., Allen, R. and Fereres, E., 2008. Integrating satellite-based evapotranspiration with simulation models for irrigation management at the scheme level. Irrigation Science, 26(3): 277-288.

Senay, G., Budde, M. and Verdin, J., 2011. Enhancing the Simplified Surface Energy Balance (SSEB) approach for estimating landscape ET: Validation with the METRIC model. Agricultural Water Management, 98(4): 606-618.

Singh, R.K. and Irmak, A., 2011. Treatment of anchor pixels in the METRIC model for improved estimation of sensible and latent heat fluxes. Hydrological Sciences Journal, 56(5): 895-906.

Singh, R.K., Irmak, A., Irmak, S. and Martin, D.L., 2008. Application of SEBAL model for mapping evapotranspiration and estimating surface energy fluxes in south-central Nebraska. Journal of irrigation and drainage engineering, 134(3): 273-285.

Su, H., McCabe, M., Wood, E., Su, Z. and Prueger, J., 2005. Modeling evapotranspiration during SMACEX: Comparing two approaches for local-and regional-scale prediction. Journal of Hydrometeorology, 6(6): 910-922.

Su, Z., 2002. The Surface Energy Balance System (SEBS) for estimation of turbulent heat fluxes. Hydrology and earth system sciences, 6(1): 85-99.

Sugita, M. and Brutsaert, W., 1991. Daily evaporation over a region from lower boundary layer profiles measured with radiosondes. Water Resources Research, 27(5): 747-752.

Tasumi, M., Allen, R.G., Trezza, R. and Wright, J.L., 2005. Satellite-based energy balance to assess within-population variance of crop coefficient curves. Journal of irrigation and drainage engineering, 131(1): 94-109.

Teixeira, A.d.C., Bastiaanssen, W., Ahmad, M.u.D. and Bos, M., 2009. Reviewing SEBAL input parameters for assessing evapotranspiration and water productivity for the Low-Middle São Francisco River basin, Brazil: Part A: Calibration and validation. Agricultural and Forest Meteorology, 149(3): 462-476.

Timmermans, W.J., Kustas, W.P., Anderson, M.C. and French, A.N., 2007. An intercomparison of the surface energy balance algorithm for land (SEBAL) and the two-source energy balance (TSEB) modeling schemes. Remote Sensing of Environment, 108(4): 369-384.

Vermote, E.F., Tanré, D., Deuze, J.L., Herman, M. and Morcette, J.-J., 1997. Second simulation of the satellite signal in the solar spectrum, 6S: An overview. IEEE transactions on geoscience and remote sensing, 35(3): 675-686.

Walter, J., Edwards, J., McDonald, G. and Kuchel, H., 2018. Photogrammetry for the estimation of wheat biomass and harvest index. Field Crops Research, 216: 165-174.

Wang, K. and Dickinson, R.E., 2012. A review of global terrestrial evapotranspiration: Observation, modeling, climatology, and climatic variability. Reviews of Geophysics, 50(2).

Yang, X. et al., 2015. Recharge and Groundwater Use in the North China Plain for Six Irrigated Crops for an Eleven Year Period. PloS one, 10(1): e0115269.